This article has been accepted for publication in a future issue of this journal, but has not been fully edited. Content may change prior to final publication. Citation information: DOI 10.1109/JSAC.2018.2864418, IEEE Journal on Selected Areas in Communications



# Cooperative UAV Cluster Assisted Terrestrial Cellular Networks for Ubiquitous Coverage

Huici Wu, Xiaofeng Tao, *Senior Member, IEEE,* Ning Zhang, *Member, IEEE,* and Xuemin (Sherman) Shen, *Fellow, IEEE*

***Abstract*—Unmanned Aerial Vehicles (UAVs), featured by flexible configuration, robust deployment, and line-of-sight links, has great potential to provide ubiquitous wireless coverage and high speed transmission. In this paper, we aim to analyze the coverage performance of UAV-assisted terrestrial cellular networks, where partially energy harvesting-powered caching UAVs are randomly deployed in the 3D space with a minimum and maximum altitude, i.e., $H_l$ and $H_h$. A novel cooperative UAV clustering scheme is proposed to offload ground mobile terminals (GMTs) from ground cellular base stations (GcBSs) to cooperative UAV clusters. A cooperative UAV cluster is developed within a cylinder with projection centered on a GMT, based on their energy states, the cached contents, and the cell loads. With tractable Poisson Point Process and Gamma approximation, explicit expressions for the successful transmission probabilities (STPs) are obtained. Theoretical analysis reveals that the cooperative probability of a UAV and the offloading probability of a GMT have bell-shaped relation with respect to the radius of the cylinder and the cache hit probability (the matching probability of a content request and content cache). Numerical results are provided to demonstrate the impacts of the system parameters on the cooperative UAV cluster. The results also give the optimal average altitude ($\frac{H_l+H_h}{2}$) and altitude difference ($H_h - H_l$) in maximizing the coverage performance with the proposed cooperative transmission scheme.**

***Index Terms*—Cooperative UAV cluster, aerial base station, stochastic geometry, gamma approximation.**

## I. Introduction

To provide flexible, dynamic and location-aware connections in next generation (5G)/beyond 5G (B5G) mobile communication networks, unmanned aerial vehicles (UAVs) are expected to be deployed in the 3D space, furnished with wireless communication modules, to provide temporally and spatially on-demand wireless connections for ground mobile terminals (GMTs), especially in urban area with dense traffic demands and in disaster circumstances [1].

Coordinating UAVs with ground cellular base stations (GcBSs) plays a key role in the UAV-assisted terrestrial networks, for enhancing network performance through traffic offloading, relaying and cooperation etc. [2], However, i) densely deployed UAVs connecting with ground control stations (GCSs) through fronthaul, for controlling, scheduling, content fetching, and information exchange etc., may cause congestions in the fronthaul link. ii) The performance of UAV-GcBS coordination is fundamentally constrained by the limited duration caused by low–capacity onboard battery of UAVs. Effective energy replenishment and management are urgently required.

UAVs with caching functionalities (defined as caching UAVs in this paper) can pre-store a part of popular contents and serve GMTs directly if the cached contents meets GMTs' requests, which eases the fronthaul congestions since it release the content fetching process from core network over fronthaul and GcBSs [3], [4]. Moreover, caching popular contents at UAVs can provide real-time and location-aware services for GMTs in an energy- and spectrum- efficient manner, through dynamic movement and cooperatively caching. Energy harvesting (EH) is an attractive technique in dealing with the constraint energy with UAVs, through exploiting energy from ambient environment such as wind and solar. Employing EH with UAVs can prolong the operational duration and thus improve the wireless connectivity [5]–[7]. EH-powered caching UAVs coexist with terrestrial cellular network, the dynamic network topology caused by the intermittent energy arrival with EH and the uncertainty of caching poses challenge on the user association between access points (APs) (including UAVs and GcBSs) and GMTs, which is key in providing robust connectivity and ubiquitous coverage in the UAV-assisted terrestrial cellular network.

In this paper, we investigate the coordination and cooperation between UAVs and GcBSs in the UAV-assisted terrestrial cellular network. The UAVs are powered by hybrid energy sources. Onboard energy, along with a part of the harvested energy, is used to maintain the flight while the rest harvested energy is used to support the communication modules at UAVs. Moreover, the UAVs proactively store a part of the most popular contents to provide direct services for GMTs if caches meet requests. GcBSs and UAVs are deployed as independent 2D Poisson Point Process (PPP) and 3D PPP, respectively. The UAVs act as aerial base stations (BSs) with a minimum and maximum altitudes, denoted as $H_l$ and $H_h$. The GcBSs and UAVs are capacity-constraint APs, i.e., the maximum number of associated GMTs with an AP is limited due to the scarcity of time-frequency-space resources. With the considered network model, a user-centric cooperative UAV

This work is supported in part by the National Key Research and Development Program of China under Grant 2017YFB0801702, in part by the National Natural Science Foundation for Distinguished Young Scholars of China under Grant 61325006, in part by the 111 Project of China under the Grant B16006, and in part by the Natural Sciences and Engineering Research Council of Canada (NSERC). *Corresponding author: Xiaofeng Tao*

H. Wu and X. Tao are with the National Engineering Lab for Mobile Network Technologies, Beijing University of Posts and Telecommunications, Beijing 100876, China (e-mail: {dailywu, taoxf}@bupt.edu.cn).

N. Zhang is with the Department of Computing Science, Texas A&M University-Corpus Christi, Corpus Christi, TX 78412 USA (e-mail: Ning.Zhang@tamucc.edu).

X. Shen is with the Department of Electrical and Computer Engineering, University of Waterloo, Waterloo, Canada (e-mail: sshen@uwaterloo.ca).

This article has been accepted for publication in a future issue of this journal, but has not been fully edited. Content may change prior to final publication. Citation information: DOI 10.1109/JSAC.2018.2864418, IEEE Journal on Selected Areas in Communications



clustering scheme is proposed to offload GMTs from GcBSs to cooperative UAVs. A cooperative UAV cluster is developed within a cylinder with projection centered at a GMTs. The energy states of the communication modules at UAVs, the matching between content caching and requesting, and the cell loads of UAVs are considered in determining a cooperative UAV. Leveraging modified Sigmoid function and dual-slope path loss model for the UAV-GMT line-of-sight (LoS) link and GcBS-GMT link, respectively, successful transmission probabilities (STPs) of the UAV-GMT link and GcBS-GMT link are obtained with Gamma approximation for the distributions of aggregated signal strength. Numerical results are further provided to validate the analytical results and demonstrate the impacts of the UAV parameters and clustering configurations on the coverage performance of the UAV-assisted terrestrial cellular network. In a nutshell, the main contributions are summarized as follows.

- We propose a user-centric cooperative UAV clustering scheme to improve the coverage performance of GMTs by traffic offloading and exploiting diversity gain.
- With the cooperative UAV clusters, offloading probability of a random GMT is obtained with the characterizations of cell load distributions of UAVs and GcBSs. Incorporating modified Sigmoid model and dual-slope path loss model for the UAV-GMT and GcBS-GMT channels, the moments and Laplace functionals of the aggregated information and interference signal strength are analyzed. Based on the results, explicit expressions for the conditional UAV- and GcBS-STP are derived by leveraging Gamma approximation for the distributions of aggregated signal strength.
- Theoretical analysis reveals that the cooperative probability of a random UAV and the offloading probability of a random GMTs have a bell-shaped relation with respect to (*w.r.t*) the radius of cooperative cylinder (defined as cooperative radius) and the cache size. Numerical results indicate that the UAV-STP is a unimodal function *w.r.t* the cooperative radius and the cache size. Moreover, optimal average altitude (i.e., $\frac{H_l+H_h}{2}$) and altitude difference (i.e., $H_h - H_l$) of the space for UAVs exist in maximizing the coverage performance with the proposed cooperative scheme.

The remainder of this paper is organized as follows. Section II overviews the related works. The system model, including the cooperative UAV clustering strategy, is presented in Section III. In Section IV, the cell load distribution and offloading probability are characterized. Then, the UAV- and GcBS-STP are analyzed in Section V. Numerical results are given in Section VI. Finally, Section VII concludes this work.

## II. Related Works

UAV-assisted cellular networking can help to provide ubiquitous coverage and high data rate services for the dense GMTs with low cost and high flexibility [8], [9]. The UAVs can act as aerial relays or BSs. Relaying UAVs forward signals for distant MTs without reliable direct links. Aerial BS provides ancillary wireless connectivity with terrestrial cellular networks, for traffic offloading or coverage improvement. An overview on the architecture, technologies, and radio propagations of the UAV-aided wireless communications was presented in [1], [2].

The improvement brought by UAV networks has been investigated with various air-to-ground analytical/simulation propagation models in urban/suburban/mountainous environments [10]–[14]. [15], [16] studied the performance of UAV connections with extensive channel measurements and system simulations. [17] simplified and approximated the propagation models with a modified Sigmoid function, for tractable analysis in the UAV communication networks. [18] investigated the optimal UAV altitude in the UAV small cell networks, based on the analysis of downlink coverage. The optimal 3D locations of UAVs and minimum number of UAVs were studied in [19] to meet the target coverage requirements. By modeling the UAV distributions as 2D binomial point process with fixed altitude, [20] derived the downlink coverage probability in a finite UAV network under nearest cell-association and Nakagami-$m$ fading. Furthermore, [21] analyzed the coverage probability in a 3D UAV network coexisting with 2D downlink cellular network and the optimal density of UAVs was obtained in maximizing the UAV network throughput.

Leveraging caching and EH at UAVs, the problem of optimal deployment of caching UAVs was studied in [3], with the consideration of MTs' locations, content requests, and mobility. [22] studied the minimization of energy consumption in a moving UAV-based mobile cloud computing system. [23] investigated the path planning strategy for solar powered UAVs with a graph based approach. [24] studied the cooperative throughput maximization problem in a cooperative network with UAVs acting as a EH-powered relay. Significant efforts have been put forward in the performance analysis and optimizations of the UAV networks, with/without caching and EH, coexisted with terrestrial cellular networks or not. Since the UAV networks are expected to coexist with terrestrial cellular networks, their coordination and cooperation should be studied to improve the performance and to balance the traffic and resources between UAVs and GcBSs. To the authors' best knowledge, there is seldom study on the coordination and cooperation for UAV-assisted terrestrial cellular network, where an effective UAV coordination and cooperation strategy is expected to achieve ubiquitous coverage and high network throughput [2], [25].

## III. System model

### A. UAV-assisted Terrestrial Cellular Network

As shown in Fig. 1(a), we consider a UAV-assisted terrestrial cellular network, where EH-powered caching UAVs, coexisted with GcBSs, are deployed in the 3D space to provide LoS connections for GMTs. The GcBSs and UAVs are distributed according to independent 2D PPP $\Phi_b \in \mathbb{R}^2$ with density $\lambda_b$ and 3D PPP $\Phi_u \in \mathbb{R}^2 \times \mathbb{R}^+$ with density $\lambda_u$. The minimum and maximum altitudes of the airspace for UAVs are defined as $H_l$ and $H_h$, respectively. The distribution of GMTs are PPP ($\Phi_t \in \mathbb{R}^2$) modeled at the ground level with density $\lambda_t$. Without loss of generality, performance analysis is conducted at a typical

This article has been accepted for publication in a future issue of this journal, but has not been fully edited. Content may change prior to final publication. Citation information: DOI 10.1109/JSAC.2018.2864418, IEEE Journal on Selected Areas in Communications



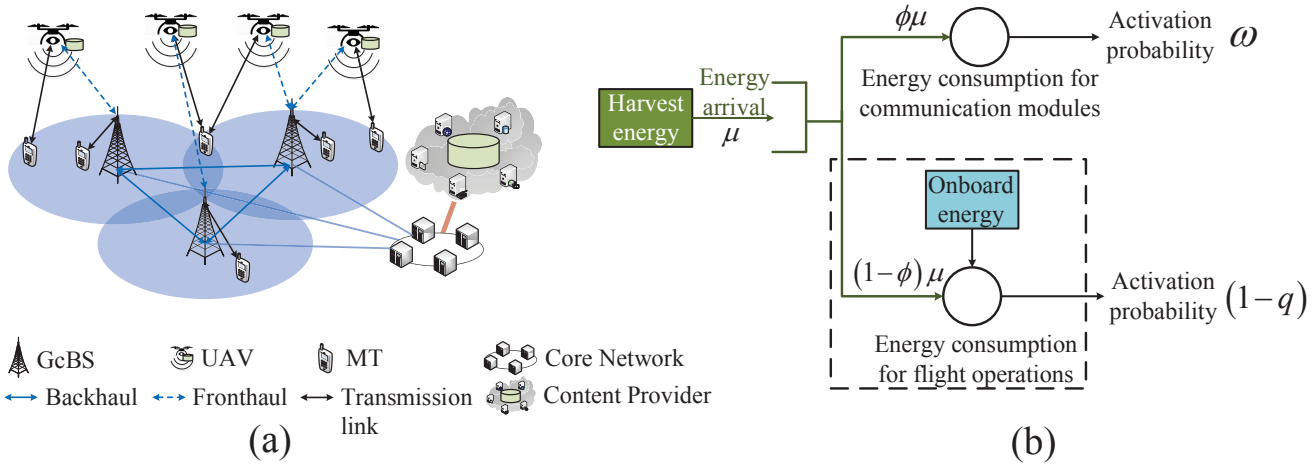


Fig. 1. UAV-assisted terrestrial cellular network and the energy harvesting model.

GMT located at the origin of the coordinate according to the Slivnyak's theorem [26], [27].

Millimeter wave (mmWave) frequency band is adopted for UAVs [28] and conventional microwave frequency band is adopted at GcBSs to mitigate inter-tier interference. Due to the scarcity of time-frequency-space resources, the connection capacities of GcBSs and UAVs, i.e., the maximum number of MTs that can be simultaneously served by a GcBS or a UAV at a time-frequency block, are defined as $N_b$ and $N_u$, respectively. Intra-cell interference is ignored with appropriate beamforming.

The UAVs are powered by hybrid energy sources, as shown in Fig. 1(b). A proportion ($\phi$) of the harvested energy is used to support the wireless communication modules[1], while the other part $(1-\phi)$, along with the onboard energy, is used to maintain the flight of UAVs. The energy consumption for flight depends on the hardware specifications of UAVs, which is not the main focus of this paper. Thus, we consider the UAVs turn off the wireless communication functionalities and go back to GCSs for energy replenishment with probability $q$. Then, all the UAVs of which the communication modules can be in operation formulate another 3D PPP with density $\lambda_u(1-q)$. Independent and identical distributed (*i.i.d.*) Bernoulli with probability $\mu$ is considered for the energy arrival process. Denote $\Delta_p$ as the amount of energy arrived in a time slot and $M$ as the minimum number of time slots required to harvest enough energy to support the communication modules. If the harvested energy is above $M\Delta_p$, the wireless communication modules will be activated and can provide wireless connections for MTs. The transmission power of GcBSs and UAVs are fixed as $P_{\text{b,tx}}$ and $P_{\text{u,tx}}$ and are uniformly allocated to the associated MTs.

[1]The communication modules equipped at UAVs can be classified as low energy–consumption aerial BSs and high energy–consumption aerial BSs. The energy consumption of low energy–consumption BSs is negligible compared to that of flight operation modules, but the energy consumption of aerial micro BSs and macro BSs is about one tenth of the energy consumption for flight operation modules. Therefore, we consider a general model in this paper and a proportion of the harvested energy is allocated to support the communication modules.

To ease the fronthaul load and to reduce latency, the UAVs pre-cache a part of popular contents at their storage such that they can serve the MTs directly if cache hits happen, i.e., the requested contents are just cached by the UAVs. Denote $\mathcal{T}=[c_1,c_2,...,c_T]$ as the content library containing $T$ contents with request probabilities $f_t, t=1,...,T$. The contents have the same size and are indexed according to request frequency. The lower indexed content has the higher popularity. *Zipf* distribution is a well-applied popularity distribution in modeling the request probability of contents. With *Zipf* model, $f_t$ is expressed as [29]:

$$f_t=\frac{1/t^{\xi}}{\sum_{i=1}^{T}1/i^{\xi}}, t\in\mathcal{T}, \tag{1}$$

where $\xi$ ($\geqslant 0$) reflects the popularity distribution skewness. The cache size of UAVs, i.e., the maximize number of contents a UAV can cache, is defined as $L$. "Most Popular Content (MPC)" scheme is adopted such that the most popular $L$ contents are prior cached at the UAVs. Each GMT makes independent requests for contents. Thus, the cache hit probability, i.e., the probability of cache hits, is $\eta=\sum_{t=1}^{L}f_t$.

### B. Radio Propagation Model

Wireless channels of transceiver links undergo path loss, small scale fading and shadow fading. Both LoS and non-line-of-sight (NLoS) propagations are considered. Since mmWave is adopted at UAVs, the effect of NLoS is dominated by that of the LoS. Thus, NLoS links can be ignored for the mmWave channel, and the path loss propagation model of the UAV-GMT links with distance $d$ can be expressed as [30], [31]:

$$l_u(d)=A_{u,0}d^{-\alpha_u}, \tag{2}$$

where $A_{u,0}$ and $\alpha_u$ are the path loss factor and exponent of the LoS link, respectively. Due to the high frequency carrier, the mmWave propagation is are very likely to be blocked by obstacles, leading to the missing of LoS link. We apply the

This article has been accepted for publication in a future issue of this journal, but has not been fully edited. Content may change prior to final publication. Citation information: DOI 10.1109/JSAC.2018.2864418, IEEE Journal on Selected Areas in Communications



TABLE I
KEY PARAMETERS AND NOTATIONS

| Symbol | Description |
|---|---|
| $\Phi_b\,(\lambda_b)$ | 2D PPP model for GcBSs with density $\lambda_b$ |
| $\Phi_u\,(\lambda_u)$ | 3D PPP model for UAVs with density $\lambda_u$ |
| $\Phi_t\,(\lambda_t)$ | PPP model for GMTs with density $\lambda_t$ |
| $P_{\text{b,tx}}$, $P_{\text{u,tx}}$ | Transmission power of GcBS and UAV |
| $H_h$, $H_l$ | The maximum and minimum altitudes for UAVs |
| $N_b$, $N_u$ | Connection capacities of GcBSs and UAVs |
| $\mu$, $M$ | Energy harvesting rate and minimum number of required time slots |
| $\xi$, $L$ | Content popularity and cache size of UAVs |

modified Sigmoid model to model the existence of blockages for the LoS in UAV-GMT links. Denote $\varphi = \arcsin\left(\frac{h}{d}\right)$ in degree as the elevation angle of a UAV-GMT link, the probability of having LoS in the UAV-GMT link is [17]

$$\Pr_u(\varphi) = \frac{1}{1 + X\exp\left(-Y\left[\varphi - X\right]\right)}, \tag{3}$$

where $X$ and $Y$ are constants depending on the environment (rural, urban, dense urban, etc.). Thus, the probability of blockage of the UAV-GMT link is $1 - \Pr_u(\varphi)$.

Small scale fading and shadow fading are considered for the UAV-GMT mmWave channel. The small scale fading of UAV-GMT mmWave channel is modeled as *i.i.d.* Gamma distribution $\mathcal{G}(\kappa, \theta)$ with shape $\kappa$ and scale $\theta$. Note that Gamma distribution is a general distribution that can be applied to characterize various channel models with different transmission techniques by selecting diverse parameters. For example, $\mathcal{G}(1,1)$ represents the Rayleigh fading gain with unit mean. $\mathcal{G}\left(m, \frac{1}{m}\right)$ represents the Nakagami-$m$ fading with parameter $m$. The shadow fading is modeled as log-normal distribution with mean 0 and variance $\delta^2$.

Define $l_{b,l}(d)$ and $l_{b,nl}(d)$ as the path loss functions of the LoS and NLoS links of GcBS-GMT channel with distance $d$. $l_{b,l}(d)$ and $l_{b,nl}(d)$ can be expressed as:

$$l_{b,l}(d) = A_{b,l}d^{-\alpha_{b,l}}, l_{b,nl}(d) = A_{b,nl}d^{-\alpha_{b,nl}}, \tag{4}$$

where $A_{b,l}$, $\alpha_{b,l}$ and $A_{b,nl}$, $\alpha_{b,nl}$ are path loss parameters for the LoS and NLoS links, respectively. Define $\Pr_{b,l}(d)$ and $\Pr_{b,nl}(d)$ as the probabilities of having LoS and NLoS in the GcBS-GMT channel, respectively. Adopting linear model [32], $\Pr_{b,l}(d)$ can be expressed as:

$$\Pr_{b,l}(d) = \begin{cases} 1 - \dfrac{d}{d_0}, 0 \leqslant d \leqslant d_0 \\ 0, d > d_0 \end{cases}, \tag{5}$$

where $d_0$ is the (distance) parameter that determines the decreasing slope of $\Pr_{b,l}(d)$. Thus, the probability of having NLoS is $\Pr_{b,nl}(d) = 1 - \Pr_{b,l}(d)$. For the small scale fading of GcBS-GMT channel, Rayleigh fading with unit mean is assumed for simplicity. Key notations and parameters are summarized as in Table I.

### C. Cooperative UAV Clustering Scheme and User Association Strategy

In this paper, we propose a cooperative UAV clustering scheme to offload GMTs from GcBSs to the nearby UAVs.

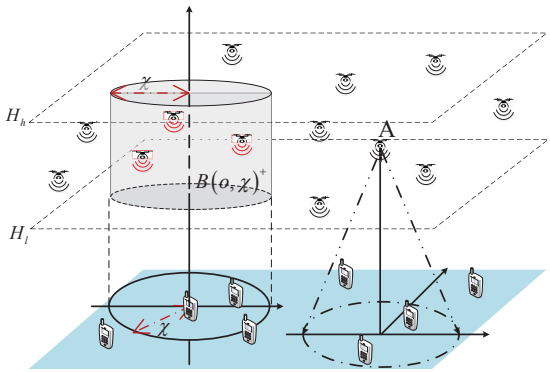


Fig. 2. Illustration of the cooperative UAV clustering.

To reduce the coordination overheads and computation, and to guarantee the efficiency of radio propagation, only the candidate UAVs in the cylinder $B(o,\chi)^+$ (seen in Fig. 2) with projection centered at the typical GMT and with radius $\chi$ have the opportunity to cooperatively serve the typical GMT. Similarly, from the UAVs' view, the association area of a UAV is a circle centered at the projection (on the ground) of the UAV and with radius $\chi$, shown as the dotted circle in Fig. 2. The GMTs inside the circle are the candidate serving GMTs of the UAV $A$.

*1) Cooperative UAV Cluster:* A candidate UAV inside $B(o,\chi)^+$ can join the cooperative cluster, to transmit the typical GMT's requested contents, only if $E_1$: it is on flight and has sufficient energy to support the communication modules, $E_2$: cache hit happens, i.e., the typical GMT's requested contents have been pre-stored at the UAV, and $E_3$: the number of other candidate serving GMTs of the UAV, defined as $n$, is less than the connection capacity of the UAV, i.e., $n < N_u$. Or else, if $n \geqslant N_u$, the candidate UAV randomly serves $N_u$ GMTs. All the candidate UAVs satisfying the above conditions are coordinated as the cooperative UAV cluster for the typical GMT.

*2) User Association:* The GMTs are associated with either the nearest GBSs or the cooperative UAV clusters. For a typical GMT, if more than one UAV satisfies the above conditions, i.e., a non-empty cooperative UAV cluster exists, the requested contents stored at cooperative UAVs are cooperatively transmitted to the GMT, similar to Coordinated multipoint (CoMP) transmission in cellular networks. With the aggregated received signal, the typical GMT performs maximum ratio combining, which can improve the received signal-to-interference-plus-noise ratio (SINR). If an empty cooperative UAV cluster exists for the typical GMT, the requested contents will be fetched over backhaul to the nearest GcBS, and then be transmitted to the typical GMT.

## IV. Cell Load Distribution and Offloading Probability

According to the cooperative clustering scheme, the cell load distribution of a UAV, i.e., the distribution of the number of GMTs associated with the UAV, is one of the keys to the

This article has been accepted for publication in a future issue of this journal, but has not been fully edited. Content may change prior to final publication. Citation information: DOI 10.1109/JSAC.2018.2864418, IEEE Journal on Selected Areas in Communications



cooperation of the UAV. Denote $p_u(i)$ as the probability that $i$ candidate GMTs are located in the association area of a UAVs, and define $\upsilon$ as the cooperative probability of a candidate UAV joining the cluster to serve the typical GMT. Then, $\upsilon$ is expressed as:

$$\begin{aligned}\upsilon &= \Pr\left(E_1 \& E_2 \& E_3\right) \\ &= (1-q)\,\omega\eta\left(\sum_{n=0}^{N_u-1} p_u(n+1) + \sum_{n=N_u}^{\infty} \frac{p_u(n+1)\,N_u}{n+1}\right),\end{aligned} \tag{6}$$

where $\omega$ is the probability of a UAV having sufficient energy to support the communication modules. Following the distributions $p_u(i)$, we define $\rho_u(m)$ as the probability that $m$ GMTs are associated with a UAV, i.e., the cell load distribution of UAVs. With the constraint of the connection capacity of UAVs, the cell load distribution of UAVs is expressed as:

$$\rho_u(m) = \begin{cases} p_u(m), m < N_u \\ \sum\limits_{i=N_u}^{\infty} p_u(i), m = N_u \end{cases} \tag{7}$$

By modeling the energy states of the communication modules as a Markov chain as in [33], [34], the energy arrival rate is $\phi\mu$ and the energy consumption rate is $\sum\limits_{m=1}^{N_u}\rho_u(m)$. Then, the probability of having sufficient energy to support the communication modules is

$$\omega = \min\left(\phi\mu \Big/ \left(M\sum_{m=1}^{N_u}\rho_u(m)\right), 1\right). \tag{8}$$

Note that $\omega = 1$ when $\phi\mu \geqslant M\sum\limits_{m=1}^{N_u}\rho_u(m)$, i.e., the energy harvesting rate is greater than the energy consumption rate, the UAVs always have sufficient energy to support the communication modules.

**Remark 1:** *The established energy harvesting and consumption model in this paper is a universal model that can be applied to the UAV communication networks with low energy-consumption aerial BSs or with high energy-consumption aerial BSs. For the scenario where UAVs carry a low energy-consumption aerial BS, the allocation factor ($\phi$) can be reduced and the minimum number of required time slots ($M$) decreases. The activation probability $\omega$ can be approximated or even equal to 1 if the energy harvesting rate is large enough. When $\omega \simeq 1$, the studied scenario is equivalent to the scenario where the communication modules are supported by onboard energy. For the scenario where UAVs carry a high energy-consumption aerial BS, the allocation factor ($\phi$), or the minimum number of required time slots ($M$), or both $\phi$ and $M$ should be increased to support the communication modules. The activation probability $\omega$ will be less than 1 with a low $\phi$ or a high $M$.*

**Remark 2:** *From the above analysis (6)-(8), we can see that there are close interactions and influences between EH, energy states of UAVs, topology of UAV network, cache scheme, selection of cooperative UAVs, and cell load of UAVs, as shown in Fig. 3. With the considered system model and the studied problem, the EH capability, along with cell load distribution of UAVs have a direct impact on the energy states of the UAVs, including the energy states for flight and communication modules. The energy states of the UAVs then influences the topology of the UAV network, which further affects the selection and determination of cooperative UAVs. Since the user association strategy is developed based on the cooperative UAV clustering scheme, the cell loads of UAVs vary with the formulation of cooperative UAV clusters.*

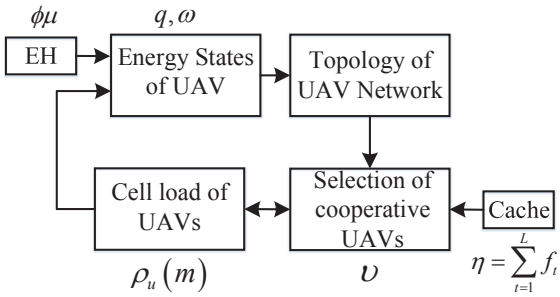


Fig. 3. Interactions and influences between the network states

With MPC adopted at UAVs, the probability $p_u(i)$ is expressed as:

$$p_u(i) = \left(\pi\chi^2\eta\lambda_t\right)^i \frac{e^{-\pi\chi^2\eta\lambda_t}}{i!}, \tag{9}$$

due to the PPP modeling of GMTs and the circular association area of UAVs. Combining with (7), the cell load distribution of a UAV with MPC is

$$\rho_u(m) = \begin{cases} \left(\pi\chi^2\eta\lambda_t\right)^m \dfrac{e^{-\pi\chi^2\eta\lambda_t}}{m!}, m < N_u \\ \dfrac{\gamma\left(N_u, \pi\chi^2\eta\lambda_t\right)}{\Gamma(N_u)}, m = N_u \end{cases} \tag{10}$$

where $\gamma(s,x) = \int\limits_0^x t^{s-1}e^{-t}\mathrm{d}t$ is the lower incomplete gamma function.

**Remark 3:** *The expressions (9)-(10) indicate that the cache hit probability and the cooperative radius have great influences on the cell load distribution of UAVs. The larger the cache size of UAVs, the higher the cache hit probability. As a result, the average cell load of UAVs becomes heavier and finally reaches the connection capacity. Similarly, the average cell load of UAVs increases with the expansion of the association area. Combining with the energy consumption and the energy harvesting model of UAVs, (8) states that the probability of having sufficient energy to support the communication modules decreases with the cache hit probability and the cooperative radius, and finally levels off to the minimum when zero-loading probability levels off to 0.*

*Moreover, according to the cooperative UAV clustering scheme, the connection capacity limits the maximum number*

This article has been accepted for publication in a future issue of this journal, but has not been fully edited. Content may change prior to final publication. Citation information: DOI 10.1109/JSAC.2018.2864418, IEEE Journal on Selected Areas in Communications



*of associated GMTs at UAVs. Thus, the under-load probability, i.e., the probability of event* $\underline{E_3}$*,*

$$\Pr\left(E_3\right)=\sum_{n=0}^{N_u-1}p_u\left(n+1\right)+\sum_{n=N_u}^{\infty}\frac{p_u\left(n+1\right)N_u}{n+1}, \quad (11)$$

*firstly increases and then decreases with the increase of the average cell load at UAVs, due to the PPP modeling of GMTs. Incorporating (6) with (8), the cooperative probability of a UAV (6) is a unimodal function* w.r.t *the cooperative radius* $\chi$ *and thus there exists a unique optimal* $\chi$ *for maximizing (6). For the cache hit probability* $\eta$*,* $\upsilon$ *is a monotonic increasing function* w.r.t $\eta$ *when* $\chi$ *is less than a critical value* $\chi_1$[2]*, below where* $\omega$ *almost remains probability* 1 *and the probability* $\Pr\left(E_3\right)$ *increases with* $\eta$*. When* $\chi$ *is above the critical value,* $\omega$ *decreases with the increase of* $\eta$*. The probability* $\Pr\left(E_3\right)$ *is a unimodal function* w.r.t $\eta$*. As a result, the cooperative probability is also a unimodal function w.r.t* $\eta$*.*

With thinning property of the PPP, the candidate UAVs in the cylinder that can join to serve the typical GMT form a 3D PPP with density $\lambda_u\upsilon$. Thus, the probability that 0 UAV participates to serve the typical GMT is

$$\vartheta=\exp\left(-\pi\chi^2\left(H_h-H_l\right)\upsilon\lambda_u\right). \quad (12)$$

If none of the candidate UAVs in the cylinder $B(o,\chi)^+$ participate to transmit the typical GMT's requested contents, the typical GMT will be served by the nearest GcBS. Therefore, $\vartheta$ also refers to the probability that a MT is served by its nearest GcBS. **Define offloading probability as the probability of a GMT being offloaded from terrestrial cellular network to UAV network. Then, the offloading probability of a random GMT is** $1-\vartheta$**.**

**Remark 4:** *(12) reveals that the probability of zero cooperative UAV depends on the density of UAVs* $\lambda_u$*, the cooperative radius* $\chi$*, the altitude difference* $H_h-H_l$*, and the cooperative probability of a candidate UAV. The offloading probability* $1-\vartheta$ *increases and finally levels off to* 1 *with denser UAVs and wider altitude difference. The probability* $\vartheta$ *approaches to* 1 *when* $\chi=0$ *and* $\chi\to+\infty$ *because the under-load probability* $\Pr\left(E_3\right)$ *and* $\upsilon$ *approach to* 0 *when* $\chi\to+\infty$*. Moreover, since* $\upsilon$ *is a unimodal function* w.r.t $\chi$*, we can get the conclusion that* $\vartheta$ *is a valley-like function* w.r.t $\chi$*.*

Since the un-offloaded GMTs are associated with GcBSs in a nearest-association way, the resulting network topology of the terrestrial cellular network is Poisson Voronoi (PV) tessellation [26]. With PPP modeling of the GMTs and with the result of Gamma approximation for the PV tessellation [35]–[37], the cell load distribution of GcBSs can be obtained as:

$$\rho_b\left(m\right)=\begin{cases}\dfrac{3.5^{3.5}\Gamma\left(m+3.5\right)}{m!\Gamma\left(3.5\right)}\dfrac{\left(\vartheta\lambda_t/\lambda_b\right)^m}{\left(3.5+\vartheta\lambda_t/\lambda_b\right)^{m+3.5}}, m<N_b\\ 1-\sum\limits_{i=0}^{N_b-1}\rho_b\left(i\right), m=N_b\end{cases}. \quad (13)$$

[2]Below where the cell load is $p_u\left(n\right)\approx 0$ when $n>N_u$.

Assuming the connection capacity of GcBSs is large enough to guarantee the wireless connections, i.e., $\lambda_b\gg\vartheta\lambda_t$, the probability of full-load at GcBs approximates to 0, i.e., $\rho_b\left(N_b\right)\approx 0$.

**Remark 5:** *Note that the theoretical analysis can be easily applied to the scenario with "Probabilistic Content Placement (PCP)" scheme. With PCP, the content* $c_t$ *is independently cached by UAVs with identical probability* $p_t$ *(*$0\leqslant p_t\leqslant 1, \sum\limits_{i=1}^{T}p_t\leqslant L$*). Thus, the cache hit probability of the PCP scheme is* $\eta_p=\sum\limits_{t=1}^{L}f_tp_t$*. According to the cache probabilities* $\{p_1,p_2,...,p_T\}$*, each UAV randomly builds a list of up to* $L$ *contents to be cached [38]. Therefore, the UAVs storing content* $c_t$ *can be modeled as a PPP with density* $p_t\lambda_u$*. Define* $p_{u,p}\left(i\right)$ *and* $\upsilon_{p,t}$ *as the probability that there are* $i$ *candidate MTs located within the association area of a UAV and the cooperative probability for a UAV joining to serve the typical GMT with requested content* $c_t$*, respectively. Then,* $p_{u,p}\left(i\right)$ *and* $\upsilon_{p,t}$ *are expressed as:*

$$p_{u,p}\left(i\right)=\left(\pi\chi^2\eta_p\lambda_t\right)^i\frac{e^{-\pi\chi^2\eta_p\lambda_t}}{i!}, \quad (14)$$

*and*

$$\upsilon_{p,t}=\left(1-q\right)\omega_pp_t\left(\sum_{n=0}^{N_u-1}p_{u,p}\left(n+1\right)+\sum_{n=N_u}^{\infty}\frac{p_{u,p}\left(n+1\right)N_u}{n+1}\right), \quad (15)$$

*respectively.* $\omega_p$ *is the probability of a UAV having sufficient energy to support the communication modules. Then, the candidate UAVs that can join to serve the typical GMT with content* $c_t$ *form a 3D PPP with density* $\lambda_u\upsilon_{p,t}$*, and the probability that* 0 *UAVs join to transmit the requested content* $c_t$ *of the typical GMT is*

$$\vartheta_{p,t}=\exp\left(-\pi\chi^2\left(H_h-H_l\right)\upsilon_{p,t}\lambda_u\right). \quad (16)$$

*With the law of total probability, the probability that* 0 *UAV participates in serving the typical GMT is* $\vartheta_p=\sum\limits_{t=1}^{T}f_t\vartheta_{p,t}$*. Thus, the expression for the cell load distribution of GcBSs with PCP has the same form as (13) by replacing (12) with* $\vartheta_p$*.*

## V. Analysis of Successful Transmission Probability

To evaluate the coverage performance of the UAV-assisted terrestrial cellular network with the proposed cooperative UAV clustering scheme, we define successful transmission probability (STP) as the probability that the received signal-to-interference-plus-noise ratio (SINR) at the typical GMT, defined as $\gamma$, is above a predetermined coverage threshold $\beta$. Then, with total probability formula, the STP can be expressed as:

$$\mathcal{P}=\Pr\left(\gamma\geqslant\beta,\ \text{GcBS associated}\right)+\Pr\left(\gamma\geqslant\beta,\ \text{UAV associated}\right). \quad (17)$$

Denote $x_0$ as the nearest GcBS to the typical GMT and denote $n_{x_0}$ and $n_{y_i}$ as the number of other candidate GMTs within the association area of $x_0$ and a UAV $y_i$, respectively.

This article has been accepted for publication in a future issue of this journal, but has not been fully edited. Content may change prior to final publication. Citation information: DOI 10.1109/JSAC.2018.2864418, IEEE Journal on Selected Areas in Communications



Denote $h_{x_0}$ as the Rayleigh fading gain of the channel between $x_0$ and the typical GMT. Denote $h_{y_i} \sim \mathcal{G}(\kappa, \theta)$ and $g_{y_i}$ as the small scale fading gain and log-normal shadowing gain between $y_i$ and the typical GMT. Define $\mathbb{1}(\text{event})$ as an indicator function with $\mathbb{1}(\text{event}) = 1$ if the event occurs, and 0 otherwise. Then, when the typical GMT is served by cooperative UAVs, the aggregated received signal strength can be expressed as:

$$S_U \triangleq \sum_{y_i \in \Phi_U \cap B(0,\chi)^+} \mathbb{1}\left(E_1 \& E_2 \& E_3\right) \frac{P_{\text{u,tx}}}{n_{y_i}+1} l_u\left(\|y_i\|\right) h_{y_i} g_{y_i}. \tag{18}$$

According to the user association strategy, the joint STPs in (17) can be expressed as:

$$\begin{aligned} &\Pr\left(\gamma \geqslant \beta, \text{ GcBS associated}\right) \\ &= \vartheta \Pr\left(\frac{P_{\text{b,tx}} l_b\left(\|x_0\|\right) h_{x_0}}{\left(n_{x_0}+1\right)\left(I_0+\sigma^2\right)} \geqslant \beta\right) \triangleq \vartheta \mathcal{P}_G, \end{aligned} \tag{19}$$

and

$$\begin{aligned} &\Pr\left(\gamma \geqslant \beta, \text{ UAV associated}\right) \\ &= (1-\vartheta) \Pr\left(\frac{S_U}{I_U+\sigma^2} \geqslant \beta\right) \triangleq (1-\vartheta) \mathcal{P}_U, \end{aligned} \tag{20}$$

where $\mathcal{P}_G$ and $\mathcal{P}_U$ are defined as the conditional UAV-STP and GcBS-STP, respectively. $\sigma^2$ is the average power of additive white Gaussian thermal noise. $I_0 = \sum_{x \in \Phi_b \setminus x_0} \frac{P_{\text{b,tx}}}{n_x} l_b\left(\|x\|\right) h_x$ is the aggregated interference strength received from other GcBSs except $x_0$. $I_U = I_{U,in} + I_{U,out}$ is the aggregated interference strength received from the interfering UAVs inside and outside $B(o,\chi)^+$.

$$\begin{aligned} I_{U,in} &= \sum_{y_j \in \Phi_U \cap B(o,\chi)^+} \mathbb{1}\left(E_1 \& !\left(E_2 \& E_3\right)\right) \frac{P_{\text{u,tx}}}{n_{y_j}} l_u\left(\|y_j\|\right) h_{y_j} g_{y_j}, \\ I_{U,out} &= \sum_{y_j \in \Phi_U \setminus B(o,\chi)^+} \mathbb{1}\left(E_1 \& \left\{n_{y_j} > 0\right\}\right) \frac{P_{\text{u,tx}}}{n_{y_j}} l_u\left(\|y_j\|\right) h_{y_j} g_{y_j}. \end{aligned} \tag{21}$$

where $!\left(E_2 \& E_3\right)$ is the opposite event of $E_2 \& E_3$.

To analyze the conditional UAV-STP $\mathcal{P}_U$ and the conditional GcBS-STP $\mathcal{P}_G$, we have to characterize the statistics of the aggregated information and interference signal strength. According to the expressions (18) and (21), it is intractable to obtain the probability density functions (*pdf*s) of $S_U$, $I_{U,in}$, $I_{U,out}$, and $I_0$ directly. However, thanks to the properties of the PPP modeling, we can obtain moments and Laplace functionals for $S_U$, $I_{U,in}$, $I_{U,out}$, and $I_0$.

**Lemma 1.** *The mean and variance of $S_U$ are expressed as:*

$$\begin{aligned} \mathbb{E}\left[S_U\right] &= 2\pi\lambda_u \kappa \theta \sqrt{e^{\delta^2}} \left(1-q\right) \omega \eta A_{u,0} P_{u,tx} \\ &\times \sum_{n=0}^{\infty} \frac{p_u\left(n+1\right)}{n+1} \int_{H_l}^{H_h} \int_{\arctan\frac{h}{\chi}}^{\pi/2} \Psi\left(2-\alpha_u\right) \mathrm{d}\varphi \mathrm{d}h, \end{aligned} \tag{22}$$

*and*

$$\begin{aligned} \mathbb{V}\left[S_U\right] &= 2\pi\lambda_u \kappa \left(\kappa+1\right) \theta^2 e^{2\delta^2} \left(1-q\right) \omega \eta (A_{u,0} P_{u,tx})^2 \\ &\times \left(\sum_{n=0}^{N_u-1} \frac{p_u\left(n+1\right)}{\left(n+1\right)^2} + \sum_{n=N_u}^{\infty} \frac{p_u\left(n+1\right)}{\left(n+1\right) N_u}\right) \\ &\times \int_{H_l}^{H_h} \int_{\arctan\frac{h}{\chi}}^{\pi/2} \Psi\left(2-2\alpha_u\right) \mathrm{d}\varphi \mathrm{d}h, \end{aligned} \tag{23}$$

*respectively, where*

$$\Psi(i) = \frac{\cot\varphi}{1 + X e^{-Y\left(\frac{180\varphi}{\pi} - X\right)}} \left(\frac{h}{\sin\varphi}\right)^i. \tag{24}$$

*Proof:* Please refer to Appendix A. ■

Eq. (24) shows that the function $\Psi(i)$ is independent of $h$ if $i = 0$, such as the case when $\alpha_u = 2$ (free space) in Eq. (22). It can be seen from (22), (23) and (6), (12) that $\mathbb{E}\left[S_U\right]$ and $\mathbb{V}\left[S_U\right]$ closely depend on the cooperative probability $\upsilon$, the cooperative radius $\chi$, and the altitude difference $H_h - H_l$. A UAV inside $B(o,\chi)^+$ interferes the typical GMT if it is energy-sufficient and events $\underline{E_2}$ and $\underline{E_3}$ are not satisfied and it has at least 1 candidate serving GMT. The probability of a energy-sufficient UAV interfering with the typical GMT is

$$\left(1-\eta\right) \sum_{n=1}^{N_u-1} p_u\left(n+1\right) + \sum_{n=N_u}^{\infty} p_u\left(n+1\right) \left(1 - \frac{\eta N_u}{n+1}\right), \tag{25}$$

which increases and finally levels off to 1 with the increase of average cell load of UAVs. For an interfering UAV outside $B(o,\chi)^+$, it interferes with the typical GMT with probability $\left(1-q\right)\omega \sum_{n=1}^{N_u} \rho_u(n)$. Thus, the means and variances of $I_{U,in}$ and $I_{U,out}$ can be obtained as follows.

**Lemma 2.** *The mean and variance of $I_{U,in}$ are expressed as:*

$$\begin{aligned} \mathbb{E}\left[I_{U,in}\right] &= 2\pi\lambda_u \kappa \theta \sqrt{e^{\delta^2}} \left(1-q\right) \omega A_{u,0} P_{u,tx} \\ &\times \left(\left(1-\eta\right) \sum_{n=1}^{N_u-1} \frac{p_u\left(n+1\right)}{n} + \sum_{n=N_u}^{\infty} \frac{p_u\left(n+1\right)}{n+1} \left(\frac{n+1}{N_u} - \eta\right)\right) \\ &\times \int_{H_m}^{H_M} \int_{\arctan\frac{h}{\chi}}^{\pi/2} \Psi\left(2-\alpha_u\right) \mathrm{d}\varphi \mathrm{d}h, \end{aligned} \tag{26}$$

*and*

$$\begin{aligned} \mathbb{V}\left[I_{U,in}\right] &= 2\pi\lambda_u \kappa \left(\kappa+1\right) \theta^2 e^{2\delta^2} \left(1-q\right) \omega (A_{u,0} P_{u,tx})^2 \\ &\times \left(\left(1-\eta\right) \sum_{n=1}^{N_u-1} \frac{p_u\left(n+1\right)}{n^2} + \sum_{n=N_u}^{\infty} \frac{p_u\left(n+1\right)}{N_u\left(n+1\right)} \left(\frac{n+1}{N_u} - \eta\right)\right) \\ &\times \int_{H_l}^{H_h} \int_{\arctan\frac{h}{\chi}}^{\pi/2} \Psi\left(2-2\alpha_u\right) \mathrm{d}\varphi \mathrm{d}h, \end{aligned} \tag{27}$$

This article has been accepted for publication in a future issue of this journal, but has not been fully edited. Content may change prior to final publication. Citation information: DOI 10.1109/JSAC.2018.2864418, IEEE Journal on Selected Areas in Communications



*respectively. The mean and variance of $I_{U,out}$ are expressed as:*

$$\mathbb{E}\left[I_{U,out}\right] = 2\pi\lambda_u\kappa\theta\sqrt{e^{\delta^2}}\left(1-q\right)\omega A_{u,0}P_{u,tx} \times \sum_{n=1}^{N_u}\frac{\rho_u\left(n\right)}{n}\int_{H_l}^{H_h}\int_{0}^{\arctan\frac{h}{\chi}}\Psi\left(2-\alpha_u\right)\mathrm{d}\varphi\mathrm{d}h, \quad (28)$$

*and*

$$\mathbb{V}\left[I_{U,out}\right] = 2\pi\lambda_u\kappa\left(\kappa+1\right)\theta^2 e^{2\delta^2}\left(1-q\right)\omega\left(A_{u,0}P_{u,tx}\right)^2 \times \sum_{n=1}^{N_u}\frac{\rho_u\left(n\right)}{n^2}\int_{H_m}^{H_M}\int_{0}^{\arctan\frac{h}{\chi}}\Psi\left(2-2\alpha_u\right)\mathrm{d}\varphi\mathrm{d}h, \quad (29)$$

*respectively.*

*Proof:* The moments of $I_{U,in}$ and $I_{U,out}$ can be easily obtained with the same derivation as $\mathbb{E}\left[S_U\right]$. ■

Eq. (22)–(26) states that the moments of $I_{U,in}$ closely depends on the probabilities (25) and $\left(1-q\right)\omega$. Combined with the discussions in **Remark 3**, (25) is an increasing function *w.r.t* the cooperative radius $\chi$. For the average interference strength $\mathbb{E}\left[I_{U,out}\right]$, since $\sum_{n=1}^{N_u}\frac{\rho_u(n)}{n}$ is a unimodal function *w.r.t* the average cell load of UAVs, $\mathbb{E}\left[I_{U,out}\right]$ has the same trend on the average cell load and $\eta$. However, with the increase of $\chi$, the average cell load of UAVs monotonically increases while the area for interfering UAVs outside $B(o,\chi)^+$ shrinks. $\mathbb{E}\left[I_{U,out}\right]=0$ when $\chi=0$ or $\chi=+\infty$, and $\mathbb{E}\left[I_{U,out}\right]>0$ when $\chi=(0,+\infty)$. According to (28) and from practical point of view, we can see that the $\mathbb{E}\left[I_{U,out}\right]$ can be maximized with a certain $\chi$.

With the moments of $S_U$, $I_{U,in}$, and $I_{U,out}$, we approximate the *pdf*s of the aggregated information and interference-plus-noise signal strength with Gamma distribution as in [39], which proved the accuracy of the second order moment matching. The Gamma distribution with the same first- and second order moments as $S_U$ has the following shape and scale parameters.

$$\kappa_{s_U} = \frac{\left(\mathbb{E}\left[S_U\right]\right)^2}{\mathbb{V}\left[S_U\right]}, \theta_{S_U} = \frac{\mathbb{V}\left[S_U\right]}{\mathbb{E}\left[S_U\right]}. \quad (30)$$

Similarly, the Gamma distribution with the same first and second order moments as $I_{U,in}+I_{U,out}+\sigma^2$ has the shape and scale parameters as:

$$\kappa_{I_U} = \frac{\left(\mathbb{E}\left[I_{U,in}\right]+\mathbb{E}\left[I_{U,out}\right]+\sigma^2\right)^2}{\mathbb{V}\left[I_{U,in}\right]+\mathbb{V}\left[I_{U,out}\right]}, \quad \theta_{I_U} = \frac{\mathbb{V}\left[I_{U,in}\right]+\mathbb{V}\left[I_{U,out}\right]}{\mathbb{E}\left[I_{U,in}\right]+\mathbb{E}\left[I_{U,out}\right]+\sigma^2}. \quad (31)$$

With the Gamma approximation, closed-form expressions for the approximated UAV-STP can be obtained as the following theorem.

**Theorem 1.** *With proposed cooperative UAV clustering scheme in the UAV-assisted terrestrial cellular networks, the conditional successful transmission probability with cooperative UAV-association is approximated as:*

$$\mathcal{P}_U \approx \frac{\left(\theta_{s_U}/\beta\theta_{I_U}\right)^{\kappa_{I_U}}}{\kappa_{I_U}B\left(\kappa_{I_U},\kappa_{s_U}\right)}{}_2F_1\left(\kappa_{I_U},\kappa_{I_U}+\kappa_{s_U};\kappa_{I_U}+1;-\frac{\theta_{s_U}}{\beta\theta_{I_U}}\right), \quad (32)$$

*where $B\left(x,y\right)$ is* Beta Euler function *and ${}_2F_1\left(a,b;c;z\right)$ is* Gauss hypergeometric function*. The conditional successful transmission probability with GcBS-association is*

$$\begin{aligned}\mathcal{P}_G \approx{}& 2\pi\lambda_b\sum_{n=0}^{N_b-2}\rho_{b,m}\left(n+1\right) \times\left(\int_0^{d_0}\frac{\mathcal{L}_{I_{0,m}}\left(\beta\left(n+1\right)\left(P_{b,tx}A_{b,l}\right)^{-1}r^{\alpha_{b,l}}\right)}{e^{\pi\lambda_b r^2+\sigma^2\beta(n+1)(P_{b,tx}A_{b,l})^{-1}r^{\alpha_{b,l}}}}\left(1-\frac{r}{d_0}\right)r\mathrm{d}r\right.\\ &+\int_0^{d_0}\frac{\mathcal{L}_{I_{0,m}}\left(\beta\left(n+1\right)\left(P_{b,tx}A_{b,nl}\right)^{-1}r^{\alpha_{b,nl}}\right)}{e^{\pi\lambda_b r^2+\sigma^2\beta(n+1)(P_{b,tx}A_{b,nl})^{-1}r^{\alpha_{b,nl}}}}\frac{r^2}{d_0}\mathrm{d}r\\ &\left.+\int_{d_0}^{\infty}\frac{\mathcal{L}_{I_{0,m}}\left(\beta\left(n+1\right)\left(P_{b,tx}A_{b,nl}\right)^{-1}r^{\alpha_{b,nl}}\right)}{e^{\pi\lambda_b r^2+\sigma^2\beta(n+1)(P_{b,tx}A_{b,nl})^{-1}r^{\alpha_{b,nl}}}}r\mathrm{d}r\right)\end{aligned} \quad (33)$$

*where $\mathcal{L}_{I_0}\left(t\right)$ is the Laplace transform of $I_0$.*

*Proof:* With Gamma approximation for the *pdf*s of aggregated information and interference-plus-noise strength, the joint UAV-STP $\mathcal{P}_U$ can be obtained by applying the result of proposition 11 in [39]. Since the typical GMT and the GcBSs are associated with the nearest manner, the *pdf* of $\|x_0\|$ is $f_{\|x_0\|}\left(r\right)=2\pi\lambda_b r e^{-\pi\lambda_b r^2}$ [26]. Then, the GcBS-STP $\mathcal{P}_G$ can be obtained as:

$$\begin{aligned}\mathcal{P}_G &= \Pr\left(h_{x_0}\geqslant\frac{\beta\left(n_{x_0}+1\right)}{P_{\mathrm{b,tx}}l_b\left(\|x_0\|\right)}\left(I_0+\sigma^2\right)\right)\\ &\overset{(b)}{\approx}\mathbb{E}_{\|x_0\|}\left[\sum_{n=0}^{N_b-2}\rho_b\left(n+1\right)\mathcal{L}_{I_0}\left(\frac{\beta\left(n+1\right)}{P_{\mathrm{b,tx}}l_b\left(r\right)}\right)e^{-\frac{\beta\sigma^2}{P_{\mathrm{b,tx}}}\frac{(n+1)}{l_b(r)}}\right],\end{aligned} \quad (34)$$

where *(b)* follows the exponential distribution of $h_{x_0}$ and the approximation $\rho_b\left(N_b\right)\approx 0$ resulting from the assumption $\lambda_b\gg\vartheta\lambda_t$. Combining with the dual-slope path loss modeling (4), (5) of $l_b\left(r\right)$, the GcBS-STP $\mathcal{P}_G$ can be obtained as (33). ■

With the dual-slope modeling of path loss propagation between GcBSs and MTs, the Laplace functional of $I_0$ in (33) are analyzed with two cases.

**Lemma 3.** *When $d_0\geqslant\|x_0\|\triangleq r$, the Laplace functional of $I_0$ is expressed as:*

$$\begin{aligned}\mathcal{L}_{I_0}\left(t\right)=\exp\left\{-\pi\lambda_b\sum_{m=1}^{N_b}\rho_b\left(m\right)\left(\mathcal{Z}\left(\alpha_{b,nl},A_{b,nl},d_0,2,m,t\right)\right.\right.\\ +\frac{2}{3}\mathcal{Y}\left(\alpha_{b,nl},A_{b,nl},d_0,3,m,t\right)-\frac{2r_0}{3d_0}\mathcal{Y}\left(\alpha_{b,nl},A_{b,nl},r_0,3,m,t\right)\\ +\mathcal{Y}\left(\alpha_{b,l},A_{b,l},d_0,2,m,t\right)-\mathcal{Y}\left(\alpha_{b,l},A_{b,l},r_0,2,m,t\right)\\ \left.\left.+\frac{2r_0}{3d_0}\mathcal{Y}\left(\alpha_{b,l},A_{b,l},r_0,3,m,t\right)-\frac{2}{3}\mathcal{Y}\left(\alpha_{b,l},A_{b,l},d_0,3,m,t\right)\right)\right\},\end{aligned} \quad (35)$$

This article has been accepted for publication in a future issue of this journal, but has not been fully edited. Content may change prior to final publication. Citation information: DOI 10.1109/JSAC.2018.2864418, IEEE Journal on Selected Areas in Communications



*where*

$$\mathcal{Z}(\alpha, A, x, n_1, n_2, t) = \frac{2x^2}{\alpha - n_1} \frac{tAP_{b,tx}}{n_2 x^\alpha} \, {}_2F_1\left(1, 1 - \frac{n_1}{\alpha}; \frac{n_1}{\alpha}; -\frac{tAP_{b,tx}}{n_2 x^\alpha}\right),$$
$$\mathcal{Y}(\alpha, A, x, n_1, n_2, t) = x^2 \, {}_2F_1\left(1, \frac{n_1}{\alpha}; 1 + \frac{n_1}{\alpha}; -\frac{n_2 x^\alpha}{tAP_{b,tx}}\right). \tag{36}$$

*When $r > d_0$, $\mathcal{L}_{I_0}(t)$ is expressed as:*

$$\mathcal{L}_{I_0}(t) = \exp\left\{-\pi\lambda_b \sum_{m=1}^{N_b} \rho_b(m) \mathcal{Z}(\alpha_{b,nl}, A_{b,nl}, r, 2, m, t)\right\}. \tag{37}$$

*Proof:* Please refer to Appendix B. ■

**Remark 6:** *For the scenario with PCP employed at UAVs, denote $\gamma_{p,U,t} = S_{p,U,t}/(I_{p,U,t,in} + I_{p,U,t,out})$ and $\gamma_{p,G,t} = \mathbb{1}(\text{GcBS associated}) \frac{l_b(\|x_0\|)h_{x_0}}{(n_{x_0}+1)(I_{0,p}+\sigma^2)}$ as the SINR received from the cooperative UAV cluster and the GcBS when content $f_t$ is requested, respectively. Define $\mathcal{P}_{p,U,t} \triangleq \Pr(\gamma_{p,U,t} \geqslant \beta)$ and $\mathcal{P}_{p,G,t} \triangleq \Pr(\gamma_{p,G,t} \geqslant \beta)$. Then, the total STP of the typical GMT is*

$$\mathcal{P}_p = \sum_{t=1}^{T} f_t(\vartheta_{p,t}\mathcal{P}_{p,U,t} + \mathcal{P}_{p,G,t}) = \sum_{t=1}^{T} f_t\vartheta_{p,t}\mathcal{P}_{p,U,t} + \mathcal{P}_{p,G}. \tag{38}$$

*The statistics of $S_{p,U,t}$, $I_{p,U,t,in}$, and $I_{p,U,t,out}$, including the mean and variance, have the same form as (22)-(23) in Lemma 1 and (26)-(29) in Lemma 2 by replacing $\eta$, $p_u(i)$, and $\omega$ with $p_t$, $p_{u,p}(i)$, and $\omega_p$, respectively. Similarly, the Laplace functional of $I_{0,p}$ has the same form as $\mathcal{L}_{I_0}(t)$ in Lemma 3 but replacing $\rho_b$ with $\rho_{b,p}$. Define*

$$\kappa_{s_{p,U,t}} = \frac{(\mathbb{E}[s_{p,U,t}])^2}{\mathbb{V}[s_{p,U,t}]}, \theta_{s_{p,U,t}} = \frac{\mathbb{V}[s_{p,U,t}]}{\mathbb{E}[s_{p,U,t}]}, \tag{39}$$

*and*

$$\kappa_{I_{p,U,t}} = \frac{(\mathbb{E}[I_{p,U,t,in}] + \mathbb{E}[I_{p,U,t,out}] + \sigma^2)^2}{\mathbb{V}[I_{p,U,t,in}] + \mathbb{V}[I_{p,U,t,out}]},$$
$$\theta_{I_{p,U,t}} = \frac{\mathbb{V}[I_{p,U,t,in}] + \mathbb{V}[I_{p,U,t,out}]}{\mathbb{E}[I_{p,U,t,in}] + \mathbb{E}[I_{p,U,t,out}] + \sigma^2}. \tag{40}$$

*Then, the approximated joint STP $\mathcal{P}_{p,U,t}$ has the same expression as (32) in Theorem 1 by replacing $\kappa_{s_U}$, $\kappa_{I_U}$, $\theta_{s_U}$, and $\theta_{I_U}$ with $\kappa_{s_{p,U,t}}$, $\kappa_{I_{p,U,t}}$, $\theta_{s_{p,U,t}}$, and $\theta_{I_{p,U,t}}$, respectively. The expression for the joint STP $\mathcal{P}_{p,G}$ has the same form as (33) by replacing $\vartheta$, $\rho_b$, and $\mathcal{L}_{I_0}(t)$ with $\vartheta_p$ , $\rho_{b,p}$, and $\mathcal{L}_{I_{0,p}}(t)$ respectively.*

## VI. Numerical and Simulation Results

In this section, we numerically evaluate the joint STPs and the total STP in the UAV-assisted terrestrial cellular network. The GcBSs are deployed with density $\lambda_b = \frac{1}{\pi 250^2}$. The UAVs are deployed in the 3D space with density $\lambda_u = \frac{15}{\pi 250^2}$. The minimum and maximum altitude UAVs are $H_l = 20$ meters and $H_h = 50$ meters. Detailed system parameters are given as in Table II unless otherwise specified.

TABLE II
System Parameters

| Parameter | Value |
|---|---|
| $\lambda_b$, $\lambda_u$, $\lambda_t$ | $\frac{1}{\pi 250^2}$, $\frac{5}{\pi 250^2}$, $\frac{15}{\pi 250^2}$ |
| $P_{\text{b,tx}}$, $P_{\text{u,tx}}$ | 37dBm, 23dBm |
| $N_b$, $N_u$ | 32, 4 |
| $H_h$, $H_l$ | 50, 20 |
| $A_{b,l}$, $\alpha_{b,l}$ | $-10.34$dB, 2.42 |
| $A_{b,nl}$, $\alpha_{b,nl}$ | $-14.54$dB, 3.75 |
| $A_{u,0}$, $\alpha_u$ | $-10.38$dB, 2.09 |
| $d_0$ $\kappa$, $\theta$ , $\delta^2$ | 0.3km, 2.5, 0.4 , 1 |
| $\xi$, $T$, $L$ | 0.8, 200, 50 |
| $q$, $\phi\mu$, $M$ | 0.2, 0.8, 5 |

The analytical results are validated in Fig. 4, where the simulation results are obtained with Monte Carlo methods in a circular area with radius 5km and $10^4$ times iterations. The cooperative radius is set as $\chi = 100$ meters. The offloading probability $(1-\vartheta)$ of the numerical result and simulation result are 0.8633 and 0.8653, respectively, which means that almost 86% of the GMTs are offloaded from GcBSs to cooperative UAV clusters. The tiny gap between the numerical results and the Monte Carlo simulations is caused by the Gamma approximation for the aggregated signal strength.

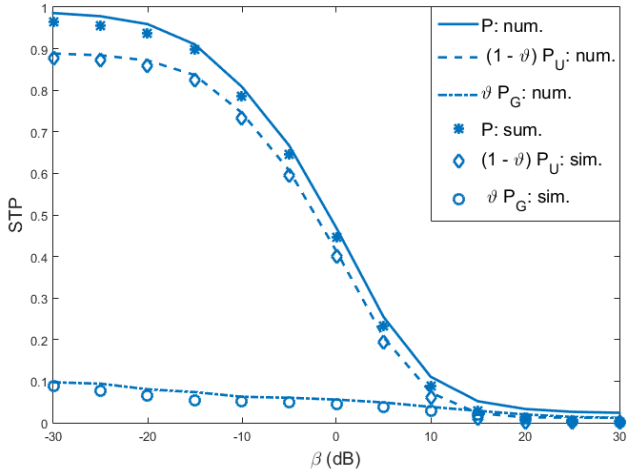


Fig. 4. STP *w.r.t.* $\beta$, $\chi = 100$m.

### A. The Impact of the Cylinder

The impact of the cooperative area, including the cooperative radius $\chi$, and the minimum and maximum altitudes $H_l$, $H_h$, is analyzed in Figs. 5-7. Fig. 5 shows the impact of $\chi$. The joint UAV-STP in Subfigure (1) and the offloading probability in Subfigure (4) show a bell-shaped relation *w.r.t.* $\chi$, which validates the theoretical analysis in Remarks. Also, we can see that the offloading probability increases and decreases sharply when $\chi$ is below or above critical values. The sharp increase is due to the widen of the cylinder and the sharp decrease is due to the heavy cell load of UAVs. For the total STP (shown in Subfigure (3)) provided by the UAV-assisted cellular network, it can be maximized with a unique cooperative threshold. Moreover, we can see from the subfigures that the GMTs are

This article has been accepted for publication in a future issue of this journal, but has not been fully edited. Content may change prior to final publication. Citation information: DOI 10.1109/JSAC.2018.2864418, IEEE Journal on Selected Areas in Communications



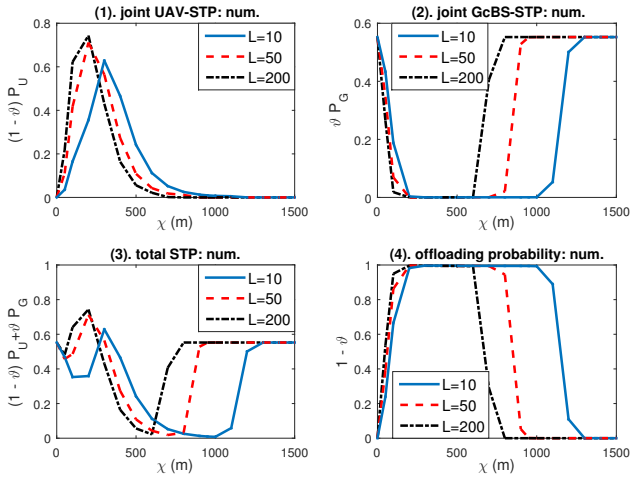


Fig. 5. STP and offloading probability *w.r.t.* $\chi$

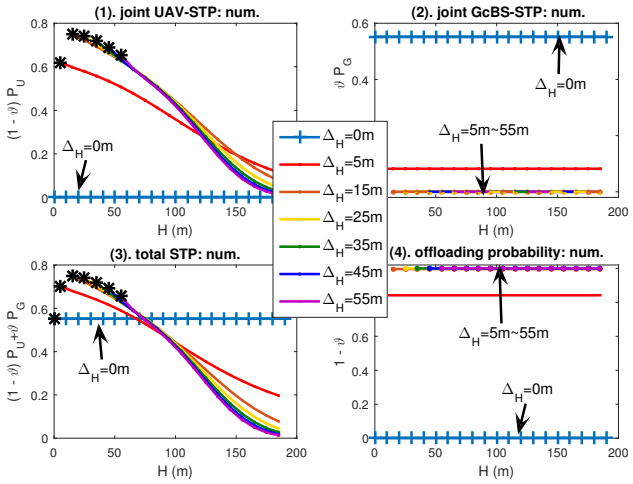


Fig. 7. STP and offloading probability *w.r.t.* $H$. $\chi = 200$m, $\beta = 0$dB.

associated with GcBSs when $\chi$ is 0m or above a certain value at which the number of candidate GMTs is much higher than the connection capacity of UAVs. In these scenarios, the GMTs are associated with the GcBSs. In conclusion, the cooperative radius should be appropriately designed with the proposed cooperative UAV clustering and user association schemes such that to balance the cell load between GcBSs and UAVs and to provide better coverage performance for GMTs.

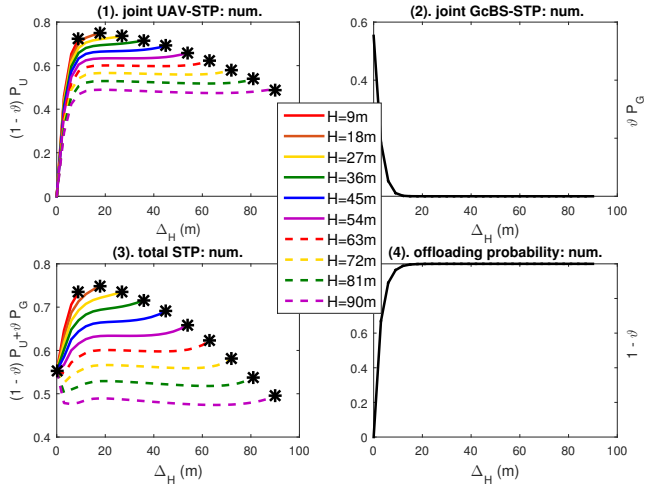


Fig. 6. STP and offloading probability *w.r.t.* $\Delta_H$. $\chi = 200$, $\beta = 0$dB.

The UAVs, elevated in the airspace, can provide LoS transmission for the GMTs. Eq. (3) indicates that the existence of LoS link depends on the altitude difference and distance of the UAV-GMT link. Define $H$ and $\Delta_H\,(\leqslant H)$ as the average altitude and half altitude difference of the UAV space, respectively. Then, the minimum and maximum altitude of the airspace for UAVs are $H_l = H - \Delta_H$ and $H_h = H + \Delta_H$.

Fig. 6 and Fig. 7 show the impact of $H$ and $\Delta_H$, respectively. It can be seen that the offloading probability increases with the enlarging of $\Delta_H$. Fig. 6 shows that the joint UAV-STP increases with the increase of $\Delta_H$, and the total STP increases with the increase of $\Delta_H$ when $H$ is less than a certain value. Fig. 7 shows that the joint UAV-STP and total STP decrease with the increase of $H$. More important, the results in Fig. 6 and Fig. 7 indicate that there is an optimal $H$ and $\Delta_H$ such that the joint UAV-STP and total STP are maximized, which means that there is an optimal vertical airspace for the UAVs with the considered cooperative UAV clustering scheme. The existence of the optimal $\Delta_H$ and $H$ is due to i) the modified Sigmoid modeling for the existence probability of LoS in the UAV-GMT link, and ii) the constraint connection capacity of UAVs. With the varying of $H$ and $\Delta_H$, there is i) a tradeoff between the existence probability of LoS and the path loss of LoS link, and ii) a tradeoff between the number of cooperative UAVs in the cylinder and the number of interfering UAVs, which results in the existence of the optimal $H$ and $\Delta_H$.

### *B. The impact of Cache Size*

A larger cache size at UAVs can pre-store more popular contents and provide higher cache hit probability, with more costs on the storage resources. Since the popularity of contents varies a lot among different contents, caching those less popular contents is less efficient than caching the more popular contents. Therefore, finding an appropriate cache size is meaningful in balancing the caching costs and the coverage improvement.

Fig. 8 presents the STP and offloading probability *w.r.t.* the cache size of UAVs. Since the cache hit probability $\eta$ monotonically increases with $L$, Fig. 8 also reveals the impact of $\eta$. The values of $\chi$ are set as 50, 150, 300, and 800 meters, which reflects light cell load, moderate cell load, and heavy cell load of UAVs.

The UAVs are light cell loaded with $\chi = 50$m and $\chi = 150$m. When $\chi = 50$m, the joint UAV-STP and the offloading probability increase slowly with $L$ (also $\eta$) due to the limited number of candidate UAVs. In this case, the increase of joint UAV-STP is less than the loss of joint GcBS-STP, and the total STP decreases. When $\chi = 150$m, the offloading probability increases and levels off to 1 rapidly the

This article has been accepted for publication in a future issue of this journal, but has not been fully edited. Content may change prior to final publication. Citation information: DOI 10.1109/JSAC.2018.2864418, IEEE Journal on Selected Areas in Communications



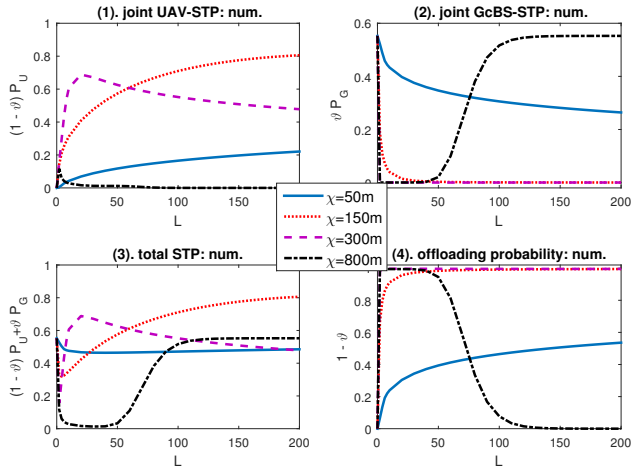


Fig. 8. STP and offloading probability *w.r.t.* $L$. $\beta = 0$dB

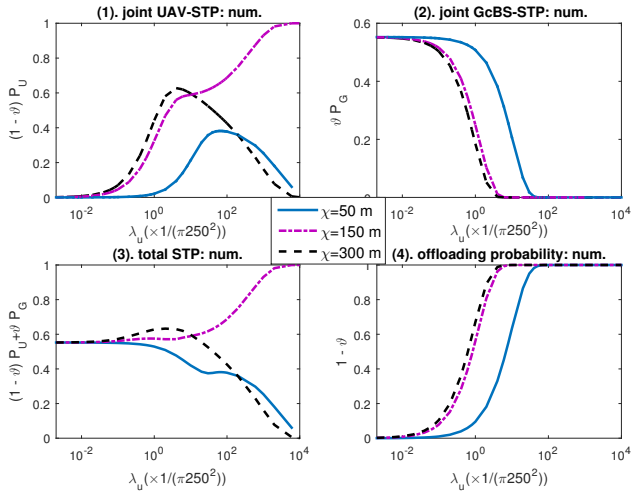


Fig. 9. STP and offloading probability *w.r.t.* $\lambda_u$. $\beta = 0$dB

increase of $L$, which results in the sharply decrease of the joint GcBS-STP. Although the joint UAV-STP monotonically increases with $L$, there is still a decrease on the total STP. With the increase of $L$, the total STP increases and finally is higher than that without UAV ($L = 0$).

The UAVs are moderately cell loaded and heavily cell loaded with $\chi = 300$m and $\chi = 800$m, respectively. The joint UAV-STP is a bell-shaped curve and a unique optimal cache size (also a unique optimal $\eta$) exists in maximizing the joint UAV-STP, which verifies the theoretical analysis in the Remarks. Moreover, Subfigure 8-(1) reveals that the optimal cache size with $\chi = 800$m is smaller than that with $\chi = 300$m. Therefore, we can get a conclusion that a smaller optimal cache hit probability is required with a larger cooperative radius, to maximize the joint UAV-STP. For the total STP, the total STP firstly decreases due to the sharp increase of the offloading probability. The decrease of the total STP is due to the fact that GMTs are offloaded to the UAVs with worse channel compared with the nearest GcBS association. However, the total STP with $\chi = 300$m can achieve a better performance than that of the system without UAVs (i.e., $L = 0$).

### C. The impact of UAV Density

The density of UAVs has a direct impact on the number of cooperative and interfering UAVs, which further influences the determination of cooperative radius. Fig. 9 shows that the offloading probability and joint GcBS-STP increases and decreases with the increase of $\lambda_u$, respectively. The joint UAV-STP is a bell-shaped curve with an optimal unique UAV density when $\chi = 50$m and $\chi = 300$m, and monotonously increases when $\chi = 150$m. The decrease of UAV-STP when $\chi = 50$m is caused by the limited cooperative radius which constraints the number of cooperative UAVs while almost does not influence the number of interfering UAVs. The decrease of UAV-STP when $\chi = 300$m is due to the relative heavy cell load of UAVs, which results in high interfering probability of UAVs. With an appropriate cooperative radius $\chi = 300$m, the

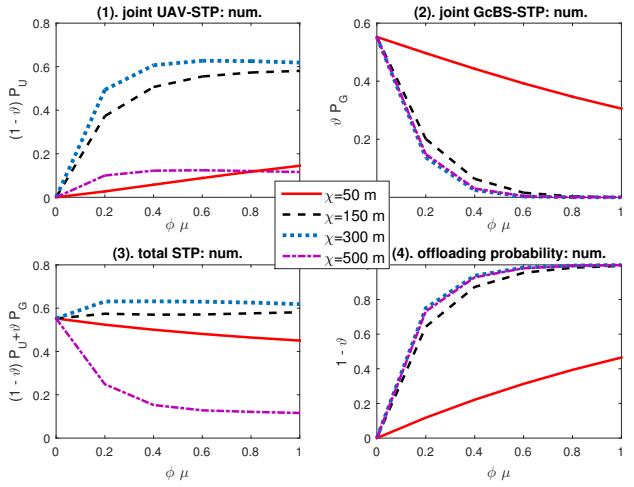


Fig. 10. STP and offloading probability *w.r.t.* $\phi\mu$. $\beta = 0$dB

number of candidate UAVs balances the interfering probability of UAV. The joint UAV-STP and total STP increases with the UAV density and finally levels off to the maximum. It can be seen from Fig. 9 (3) that there exists an optimal UAV density in maximizing the total STP when the cooperative radius is 300 meters.

### D. The impact of EH Rate

To investigate the impact of the activation of communication modules at UAVs, Fig. 10 shows the STP and offloading probability *w.r.t.* the energy arrival rate $\phi\mu$. The results show that the joint UAV-STP and offloading probability increases with $\phi\mu$ while the joint GcBS-STP decreases with $\phi\mu$. The increases and decrease final level off to maximum and minimum due to the minimum function in (8). When $\chi = 50$m and $\chi = 500$m, the total STP decreases with $\phi\mu$. The decrease with $\chi = 50$m and $\chi = 500$m is due to the limited number of candidate UAVs and the heavy cell load, respectively. When $\chi = 150$m and

This article has been accepted for publication in a future issue of this journal, but has not been fully edited. Content may change prior to final publication. Citation information: DOI 10.1109/JSAC.2018.2864418, IEEE Journal on Selected Areas in Communications



$\chi = 300$m, the increase of joint UAV-STP is greater than the decrease of joint GcBS-STP and thus the total STP increases.

In summary, from the theoretical and numerical analyses, there exists an optimal cylindric cooperative area, including an optimal cooperative radius, average altitude, and altitude difference, for the aerial UAVs such that the joint UAV-STP is maximized. With determined cylindric cooperative area, a unique optimal cache size and UAV density exist in balancing the number of cooperative UAVs and the interfering probability of a UAV, and hence maximizing the joint UAV-STP. Moreover, we can see that with the increase of the number of candidate UAVs, more MTs are offloaded to the cooperative UAV clusters. Excessive offloading deteriorates the overall performance because i) the GMTs may be offloaded to the UAVs with worse channel conditions than that with the nearest GcBSs, and ii) the GMTs are congested with over cell-loaded UAVs. Therefore, designing optimal system parameters for the deployment of UAVs and setting appropriate configurations for the cooperative UAV clustering are of significance in the UAVs-assisted terrestrial cellular network.

## VII. Conclusion

In this paper, we have studied the coverage performance of cooperative UAV clustering in the terrestrial cellular networks with EH-powered caching UAVs. A user-centric cooperative UAV clustering scheme was proposed, and the successful transmission probabilities for a random GMT were derived with Gamma approximations for the aggregated signal strength. Theoretical and numerical results have revealed an optimal cooperative radius, an optimal average altitude, and an optimal altitude difference in maximizing the coverage performance of the cooperative UAV cluster assisted terrestrial network. Moreover, with appropriate cooperative cylinder, there exists an optimal cache size and UAV density in maximizing the coverage performance of the system. The results in this paper provide theoretical insights for the deployment of UAVs and the configuration of coordination and cooperation among UAV for future terrestrial cellular network and airborne networks.

## Appendix A
## Proof of Lemma 1

Applying the expression (2-19) in [26], the mean of $S_U$ can be derived as:

$$\begin{aligned}\mathbb{E}\left[S_U\right] &= \mathbb{E}\left[\sum_{y_i\in\Phi_U\cap B(o,\chi)^+} \mathbb{1}\left(E_1\&E_2\&E_3\right)\frac{P_{\text{u,tx}} l_u\left(\|y_i\|\right) h_{y_i} g_{y_i}}{n_{y_i}+1}\right] \\ &= \mathbb{E}\left(h\right)\mathbb{E}\left(g\right) 2\pi\lambda_u P_{\text{u,tx}} \\ &\times \int_{H_m}^{H_M}\int_0^{\chi} \mathbb{E}\left(\mathbb{1}\left(E_1\&E_2\&E_3\right)\frac{l_u\left(\sqrt{r^2+h^2}\right)}{n+1}\right) r\mathrm{d}r\mathrm{d}h \\ &\overset{(e)}{=} \theta\kappa\sqrt{e^{\delta^2}} 2\pi\lambda_u\left(1-q\right)\omega\eta A_{u,0} P_{\text{u,tx}} \\ &\times \left(\sum_{n=0}^{N_u-1} p_u\left(n+1\right)\int_{H_m}^{H_M}\int_0^{\chi}\Pr_u\left(\varphi\right)\frac{\left(\sqrt{r^2+h^2}\right)^{-\alpha_u}}{n+1} r\mathrm{d}r\mathrm{d}h \right. \\ &\left. + \sum_{n=N_u}^{\infty}\frac{p_u\left(n+1\right)N_u}{n+1}\int_{H_l}^{H_h}\int_0^{\chi}\Pr_u\left(\varphi\right)\frac{\left(\sqrt{r^2+h^2}\right)^{-\alpha_u}}{N_u} r\mathrm{d}r\mathrm{d}h\right),\end{aligned} \tag{41}$$

where *(e)* is obtained by taking expectation over cell load distribution and LoS path loss. Applying (3) and replacing $r$ with $h/\tan\varphi$, the mean of $S_U$ is obtained as (22). The variance of $S_U$ is

$$\begin{aligned}&\mathbb{V}\left[S_U\right] = \mathbb{E}\left[S_U^2\right] - \left(\mathbb{E}\left[S_U\right]\right)^2 \\ &\overset{(f)}{=} \left(P_{\text{u,tx}}\right)^2\mathbb{E}\left(h^2\right)\mathbb{E}\left(g^2\right) 2\pi\lambda_u \\ &\times \int_{H_l}^{H_h}\int_0^{\chi}\mathbb{E}\left(\mathbb{1}\left(E_1\&E_2\&E_3\right)\left(\frac{l_u\left(\sqrt{r^2+h^2}\right)}{n+1}\right)^2\right) r\mathrm{d}r\mathrm{d}h,\end{aligned} \tag{42}$$

where *(f)* follows the result (2-21) in [26]. Taking the expectation over cell load distribution and LoS path loss as in (41), the variance of $S_U$ can be obtained as (23).

## Appendix B
## Proof of Lemma 4

When $d_0 \geqslant \|x_0\| \triangleq r$, the Laplace functional of $I_0$ with the dual-slope modeling of path loss (4), (5) is

$$\begin{aligned}\mathcal{L}_{I_0}(t) = &\exp\left\{-2\pi\lambda_b\int_r^{d_0}\left[\frac{x}{d_0}\left(1-\mathbb{E}_{h,n}\left[e^{-\frac{t}{n}P_{\text{b,tx}}A_{b,nl}x^{-\alpha_{b,nl}}h}\right]\right)\right.\right. \\ &\left.\left.+\left(1-\frac{x}{d_0}\right)\left(1-\mathbb{E}_{h,n}\left[e^{-\frac{t}{n}P_{\text{b,tx}}A_{b,l}x^{-\alpha_{b,l}}h}\right]\right)\right] x\mathrm{d}x\right\} \\ &\times\exp\left\{-2\pi\lambda_b\int_{d_0}^{\infty}\left(1-\mathbb{E}_{h,n}\left[e^{-\frac{t}{n}P_{\text{b,tx}}A_{b,nl}x^{-\alpha_{b,nl}}h}\right]\right) x\mathrm{d}x\right\} \\ \overset{(g)}{=}&\exp\left\{-2\pi\lambda_b\sum_{n=1}^{N_b}\rho_b\left(n\right)\int_r^{d_0}\left[\frac{x}{d_0}\left(1+\frac{n}{tP_{\text{b,tx}}A_{b,nl}x^{-\alpha_{b,nl}}}\right)^{-1}\right.\right. \\ &\left.\left.+\left(1-\frac{x}{d_0}\right)\left(1+\frac{n}{tP_{\text{b,tx}}A_{b,l}x^{-\alpha_{b,l}}}\right)^{-1}\right] x\mathrm{d}x\right\} \\ &\times\exp\left\{-2\pi\lambda_b\sum_{m=1}^{N_b}\rho_b\left(n\right)\int_{d_0}^{\infty}\left(1+\frac{n}{tP_{\text{b,tx}}A_{b,nl}x^{-\alpha_{b,nl}}}\right)^{-1} x\mathrm{d}x\right\}\end{aligned} \tag{43}$$

where (g) is the result of the exponential distribution of $h$. Replacing $y = \frac{n}{tP_{\text{b,tx}}A_{b,l}}x^{\frac{\alpha_{b,l}}{2}}$ and $y = \frac{n}{tP_{\text{b,tx}}A_{b,nl}}x^{\frac{\alpha_{b,nl}}{2}}$, the integrals in (43) can be calculated and $\mathcal{L}_{I_0}(t)$ can be obtained as (35).

When $r > d_0$, the Laplace functional of $I_0$ is

$$\begin{aligned}\mathcal{L}_{I_0}(t) = &\exp\left\{-2\pi\lambda_b\right. \\ &\left.\times\sum_{n=1}^{N_b}\rho_b\left(n\right)\int_r^{\infty}\left(1+\frac{n}{tP_{\text{b,tx}}A_{b,nl}x^{-\alpha_{b,nl}}}\right)^{-1} x\mathrm{d}x\right\}.\end{aligned} \tag{44}$$

With the similar manipulation as in (43), (44) can be further derived as (37).

## REFERENCES


[1] L. Afonso, N. Souto, P. Sebastiao, M. Ribeiro, T. Tavares, and R. Marinheiro, "Cellular for the skies: exploiting mobile network infrastructure for low altitude air-to-ground communications," *IEEE Aerosp. Electron. Syst. Mag.*, vol. 31, no. 8, pp. 4–11, Aug. 2016.

[2] Y. Zeng, R. Zhang, and T. J. Lim, "Wireless communications with unmanned aerial vehicles: opportunities and challenges," *IEEE Commun. Mag.*, vol. 54, no. 5, pp. 36–42, May. 2016.

[3] M. Chen, M. Mozaffari, W. Saad, C. Yin, M. Debbah, and C. S. Hong, "Caching in the sky: Proactive deployment of cache-enabled unmanned aerial vehicles for optimized quality-of-experience," *IEEE J. Sel. Areas Commun.*, vol. 35, no. 5, pp. 1046–1061, May. 2017.

[4] E. K. Markakis, K. Karras, A. Sideris, G. Alexiou, and E. Pallis, "Computing, caching, and communication at the edge: The cornerstone for building a versatile 5G ecosystem," *IEEE Commun. Mag.*, vol. 55, no. 11, pp. 152–157, Nov. 2017.

[5] R. Sowah, M. A. Acquah, A. R. Ofoli, G. A. Mills, and K. M. Koumadi, "Rotational energy harvesting to prolong flight duration of quadcopters," *IEEE Trans. Ind. Appl.*, vol. 53, no. 5, pp. 4965–4972, Apr. 2017.

[6] A. Alsharoa, H. Ghazzai, A. Kadri, and A. E. Kamal, "Energy management in cellular hetnets assisted by solar powered drone small cells," in *IEEE Wireless Communications and Networking Conference (WCNC)*, May 2017, pp. 1–6.

[7] Y. Dong, J. Cheng, M. Hossain, V. Leung *et al.*, "Extracting the most weighted throughput in uav empowered wireless systems with nonlinear energy harvester," *arXiv preprint arXiv:1804.10723*, 2018.

[8] Y. Li and L. Cai, "UAV-assisted dynamic coverage in a heterogeneous cellular system," *IEEE Network*, vol. 31, no. 4, pp. 56–61, Jul. 2017.

[9] N. Zhang, S. Zhang, P. Yang, O. Alhussein, W. Zhuang *et al.*, "Software defined space-air-ground integrated vehicular networks: Challenges and solutions," *IEEE Commun. Mag.*, vol. 55, no. 7, pp. 101–109, Jul. 2017.

[10] A. Al-Hourani, S. Kandeepan, and A. Jamalipour, "Modeling air-to-ground path loss for low altitude platforms in urban environments," in *IEEE Global Communications Conference (GLOBECOM)*, Dec. 2014, pp. 2898–2904.

[11] D. W. Matolak and R. Sun, "Air–ground channel characterization for unmanned aircraft systemsłpart I: Methods, measurements, and models for over-water settings," *IEEE Trans. Veh. Technol.*, vol. 66, no. 1, pp. 26–44, Jan. 2017.

[12] R. Sun and D. W. Matolak, "Air–ground channel characterization for unmanned aircraft systems part II: Hilly and mountainous settings," *IEEE Trans. Veh. Technol.*, vol. 66, no. 3, pp. 1913–1925, Mar. 2017.

[13] D. W. Matolak and R. Sun, "Air-ground channel characterization for unmanned aircraft systemsłpart III: The suburban and near-urban environments," *IEEE Trans. Veh. Technol.*, vol. 66, no. 8, pp. 6607–6618, Aug. 2017.

[14] R. Amorim, H. Nguyen, P. Mogensen, I. Z. Kovács, J. Wigard, and T. B. Sørensen, "Radio channel modeling for UAV communication over cellular networks," *IEEE Wireless Commun. Lett.*, vol. 6, no. 4, pp. 514–517, Apr. 2017.

[15] H. C. Nguyen, R. Amorim, J. Wigard, I. Z. Kovács, T. B. Sørensen, and P. E. Mogensen, "How to ensure reliable connectivity for aerial vehicles over cellular networks," *IEEE Access*, vol. 6, pp. 12 304–12 317, 2018.

[16] X. Lin, V. Yajnanarayana, S. D. Muruganathan, S. Gao, H. Asplund, H.-L. Maattanen, M. Bergstrom, S. Euler, and Y.-P. E. Wang, "The sky is not the limit: LTE for unmanned aerial vehicles," *IEEE Communications Magazine*, vol. 56, no. 4, pp. 204–210, Apr. 2018.

[17] A. Al-Hourani, S. Kandeepan, and S. Lardner, "Optimal LAP altitude for maximum coverage," *IEEE Wireless Commun. Lett.*, vol. 3, no. 6, pp. 569–572, Jun. 2014.

[18] M. Mozaffari, W. Saad, M. Bennis, and M. Debbah, "Drone small cells in the clouds: Design, deployment and performance analysis," in *IEEE Global Communications Conference (GLOBECOM)*, San Diego, CA, USA, Dec. 2015, pp. 1–6.

[19] ——, "Efficient deployment of multiple unmanned aerial vehicles for optimal wireless coverage," *IEEE Commun. Lett.*, vol. 20, no. 8, pp. 1647–1650, Aug. 2016.

[20] V. V. Chetlur and H. S. Dhillon, "Downlink coverage analysis for a finite 3D wireless network of unmanned aerial vehicles," *IEEE Trans. Commun.*, vol. 65, no. 10, pp. 4543–4558, Oct. 2017.

[21] C. Zhang and W. Zhang, "Spectrum sharing for drone networks," *IEEE J. Sel. Areas Commun.*, vol. 35, no. 1, pp. 136–144, Jan. 2017.

[22] S. Jeong, O. Simeone, and J. Kang, "Mobile edge computing via a UAV-mounted cloudlet: Optimization of bit allocation and path planning," *IEEE Trans. Veh. Technol.*, vol. 67, no. 3, pp. 2049–2063, Mar. 2018.

[23] R. Dai, "Path planning of solar-powered unmanned aerial vehicles at low altitude," in *IEEE International Midwest Symposium on Circuits and Systems (MWSCAS)*, Dec. 2013, pp. 693–696.

[24] S. Yin, J. Tan, and L. Li, "UAV-assisted cooperative communications with wireless information and power transfer," *arXiv preprint arXiv:1710.00174*, Oct. 2017.

[25] S. Sekander, H. Tabassum, and E. Hossain, "Multi-tier drone architecture for 5G/B5G cellular networks: Challenges, trends, and prospects," *IEEE Commun. Mag.*, vol. 56, no. 3, pp. 96–103, Mar. 2018.

[26] F. Baccelli and B. Blaszczyszyn, *Stochastic Geometry and Wireless Networks: Volume I-Theory*. Massachusetts: Now Publishers, 2009.

[27] Q. Cui, X. Yu, Y. Wang, and M. Haenggi, "The SIR meta distribution in poisson cellular networks with base station cooperation," *IEEE Trans. Commun.*, vol. 66, no. 3, pp. 1234–1249, 2018.

[28] L. Kong, L. Ye, F. Wu, M. Tao, G. Chen, and A. V. Vasilakos, "Autonomous relay for millimeter-wave wireless communications," *IEEE J. Sel. Areas Commun.*, vol. 35, no. 9, pp. 2127–2136, 2017.

[29] X. Wang, M. Chen, T. Taleb, A. Ksentini, and V. C. M. Leung, "Cache in the air: Exploiting content caching and delivery techniques for 5G systems," *IEEE Trans. Commun. Mag.*, vol. 52, no. 2, pp. 131–139, Feb. 2014.

[30] Z. Ding, P. Fan, and H. V. Poor, "Random beamforming in millimeter-wave NOMA networks," *IEEE Access*, vol. 5, pp. 7667–7681, Feb. 2017.

[31] G. Lee, Y. Sung, and J. Seo, "Randomly-directional beamforming in millimeter-wave multiuser MISO downlink," *IEEE Trans. Wireless Commun.*, vol. 15, no. 2, pp. 1086–1100, Feb. 2016.

[32] M. Ding, P. Wang, D. López-Pérez, G. Mao, and Z. Lin, "Performance impact of LoS and NLoS transmissions in dense cellular networks," *IEEE Trans. Wireless Commun.*, vol. 15, no. 3, pp. 2365–2380, Mar. 2016.

[33] P. Yu, J. Lee, T. Q. S. Quek, and Y. P. Hong, "Traffic offloading in heterogeneous networks with energy harvesting personal cells-network throughput and energy efficiency," *IEEE Trans. Wireless Commun.*, vol. 15, no. 2, pp. 1146–1161, Feb. 2016.

[34] H. Wu, X. Tao, N. Zhang, D. Wang, S. Zhang, and X. Shen, "On base station coordination in cache-and energy harvesting-enabled hetnets: A stochastic geometry study," *IEEE Trans. Commun.*, 2017.

[35] J. S. Ferenc and Z. Néda, "On the size distribution of poisson voronoi cells," *Phys. A: Stat. Mech. Appl.*, vol. 385, no. 2, pp. 519–529, 2007.

[36] T. Kiang, "Random fragmentation in two and three dimensions," *Zeitschrift fur Astrophysik*, vol. 64, p. 433, 1966.

[37] H. S. Dhillon and J. G. Andrews, "Downlink rate distribution in heterogeneous cellular networks under generalized cell selection," *IEEE Wireless Commun. Lett.*, vol. 3, no. 1, pp. 42–45, Jan. 2014.

[38] B. Blaszczyszyn and A. Giovanidis, "Optimal geographic caching in cellular networks," in *IEEE International Conference on Communications (ICC)*, May. 2015, pp. 3358–3363.

[39] H. Robert W, M. Kountouris, and T. Bai, "Modeling heterogeneous network interference using poisson point processes," *IEEE Trans. Signal Process.*, vol. 61, no. 16, pp. 4114–4126, May. 2013.


**Huici Wu** received her B.S. degree in communication engineering from Communication University of China, Beijing, China, in 2013, and received her Ph.D. degree in information and communication engineering from Beijing University of Posts and Telecommunications (BUPT), Beijing, China, in 2018. From September 2016 to August 2017, she is visiting the Broadband Communications Research (BBCR) Group, Department of Electrical and Computer Engineering, University of Waterloo, Waterloo, ON, Canada. She is now an assistant professor in the School of Cyberspace Security in BUPT. Her research interests are in the area of wireless communications and networks, with current emphasis on the cooperation and physical layer security in heterogeneous networks.

This article has been accepted for publication in a future issue of this journal, but has not been fully edited. Content may change prior to final publication. Citation information: DOI 10.1109/JSAC.2018.2864418, IEEE Journal on Selected Areas in Communications



**Xiaofeng Tao** (SM'13) received the B.S. degree in electrical engineering from Xi'an Jiaotong University, Xi'an, China, in 1993 and the M.S.E.E. and Ph.D. degrees in telecommunication engineering from the Beijing University of Posts and Telecommunications (BUPT), Beijing, China, in 1999 and 2002, respectively.

He was a Visiting Professor with Stanford University, Stanford, CA, USA, from 2010 to 2011; the Chief Architect of the Chinese National FuTURE Fourth-Generation (4G) TDD working group from 2003 to 2006; and established the 4G TDD CoMP trial network in 2006. He is currently a Professor with the BUPT and a Fellow of the Institution of Engineering and Technology. He is the inventor or coinventor of 50 patents and the author or coauthor of 120 papers in 4G and beyond 4G.

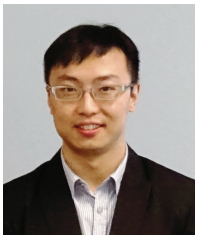

**Ning Zhang** (M'15) received the Ph.D degree from University of Waterloo in 2015. He is now an assistant professor in the Department of Computing Science at Texas A&M University-Corpus Christi. Before that, he was a postdoctoral research fellow at BBCR lab in University of Waterloo. He was the co-recipient of the Best Paper Award at IEEE GLOBECOM 2014 and IEEE WCSP 2015. His current research interests include next generation wireless networks, software defined networking, vehicular networks, and physical layer security.

**Xuemin (Sherman) Shen** (M'97-SM'02-F'09) received the B.Sc.(1982) degree from Dalian Maritime University (China) and the M.Sc. (1987) and Ph.D. degrees (1990) from Rutgers University, New Jersey (USA), all in electrical engineering. He is a University Professor and the Associate Chair for Graduate Studies, Department of Electrical and Computer Engineering, University of Waterloo, Canada. Dr. Shens research focuses on resource management, wireless network security, social networks, smart grid, and vehicular ad hoc and sensor networks. He was an elected member of IEEE ComSoc Board of Governor, and the Chair of Distinguished Lecturers Selection Committee. Dr. Shen served as the Technical Program Committee Chair/Co-Chair for IEEE Globecom16, Infocom14, IEEE VTC10 Fall, and Globecom07, the Symposia Chair for IEEE ICC10, the Tutorial Chair for IEEE VTC11 Spring and IEEE ICC08, the General Co-Chair for ACM Mobihoc15, Chinacom07 and QShine06, the Chair for IEEE Communications Society Technical Committee on Wireless Communications, and P2P Communications and Networking. He also serves/served as the Editor-in-Chief for IEEE Internet of Things Journal, IEEE Network, Peer-to-Peer Networking and Application, and IET Communications; a Founding Area Editor for IEEE Transactions on Wireless Communications; an Associate Editor for IEEE Transactions on Vehicular Technology, Computer Networks, and ACM/Wireless Networks, etc.; and the Guest Editor for IEEE JSAC, IEEE Wireless Communications, IEEE Communications Magazine, and ACM Mobile Networks and Applications, etc. Dr. Shen received the Excellent Graduate Supervision Award in 2006, and the Premiers Research Excellence Award (PREA) in 2003 from the Province of Ontario, Canada. Dr. Shen is a registered Professional Engineer of Ontario, Canada, an IEEE Fellow, an Engineering Institute of Canada Fellow, a Canadian Academy of Engineering Fellow, a Royal Society of Canada Fellow, and a Distinguished Lecturer of IEEE Vehicular Technology Society and Communications Society.